



## RESEARCH LETTER

10.1029/2018GL077664

### Key Points:

- The seasonal footprinting (SF) mechanism is a key to ENSO complexity and asymmetry, but the charged-discharged (CD) mechanism reduces them
- The CMIP5 models overestimate (underestimate) the strength of the CD (SF) mechanism, causing their simulated ENSOs to be too regular
- The strength of CD mechanism has been steady, but SF mechanism has intensified during the past two decades, making ENSO more complicated

### Supporting Information:

- Supporting Information S1
- Figure S1
- Figure S2
- Figure S3
- Figure S4
- Figure S5
- Figure S6
- Figure S7
- Figure S8

### Correspondence to:

J.-Y. Yu,  
jyyu@uci.edu

### Citation:

Yu, J.-Y., & Fang, S.-W. (2018). The distinct contributions of the seasonal footprinting and charged-discharged mechanisms to ENSO complexity. *Geophysical Research Letters*, 45. <https://doi.org/10.1029/2018GL077664>

Received 26 FEB 2018

Accepted 22 JUN 2018

Accepted article online 28 JUN 2018

## The Distinct Contributions of the Seasonal Footprinting and Charged-Discharged Mechanisms to ENSO Complexity

Jin-Yi Yu<sup>1</sup> and Shih-Wei Fang<sup>1</sup>

<sup>1</sup>Department of Earth System Science, University of California, Irvine, CA, USA

**Abstract** This study finds the seasonal footprinting (SF) mechanism to be a key source of El Niño–Southern Oscillation (ENSO) complexity, whereas the charged-discharged (CD) mechanism acts to reduce complexity. The CD mechanism forces El Niño and La Niña to follow each other, resulting in a more cyclic and less complex ENSO evolution, while the SF mechanism involves subtropical forcing and results in an ENSO evolution that is more episodic and irregular. The SF mechanism also has a tendency to produce multiyear La Niña events but not multiyear El Niño events, contributing to El Niño–La Niña asymmetries. The strength of CD mechanism has been steady, but SF mechanism has intensified during the past two decades, making ENSO more complicated. Most Climate Model Intercomparison Project version 5 models overestimate the strength of the CD mechanism but underestimate the strength of the SF mechanism, causing their simulated ENSOs to be too regular and symmetric.

**Plain Language Summary** El Niño–Southern Oscillation (ENSO) is known to have profound climate impacts worldwide, but the causes of its complex behaviors are still not fully understood. In this study, we show that the subtropical atmosphere–ocean coupled forcing is a key source of ENSO complexity, whereas the tropical ocean heat content variation acts to reduce ENSO complexity. The subtropical forcing also has a tendency to produce multiyear La Niña events but not multiyear El Niño events, contributing to El Niño–La Niña asymmetries. In contrast to the steady strength of the tropical variation throughout the past six decades, the strength of the subtropical forcing has increased since the early 1990s. This may have made ENSO more complex recently and, if this trend does not reverse, possibly into the coming decades. Contemporary climate models overestimate the strength of the tropical ocean heat content variation but underestimate the strength of the subtropical forcing, which may be a reason why contemporary models produce ENSO behavior that is too regular.

## 1. Introduction

Not all El Niño–Southern Oscillation (ENSO) events are the same. Some noticeable changes in ENSO properties observed during recent decades have motivated efforts to better understand the sources/causes of ENSO complexity (Capotondi et al., 2015; Wang et al., 2017). A significant component of ENSO complexity is manifested in the way one ENSO event transitions to another. Some events are followed by events of the opposite phase (i.e., El Niño to La Niña or La Niña to El Niño) to give rise to ENSO cycles; others are followed by neutral years to become episodic events, and still others are followed by events of the same phase to become multiyear El Niño or La Niña events. In this study, we examine how the different onset mechanisms of ENSO may affect these event-to-event transitions and thus ENSO complexity.

Studies on ENSO dynamics have identified two key onset mechanisms for events: the charged-discharged (CD) and seasonal footprinting (SF) mechanisms. The CD mechanism describes how the lagged response of the equatorial Pacific thermocline to ENSO wind forcing can result in alternations between El Niño and La Niña phases (Jin, 1997a, 1997b; Wyrski, 1975). The SF mechanism describes how subtropical Pacific sea surface temperature (SST) anomalies initially induced by atmospheric disturbances can be sustained through several seasons and, at the same time, spread equatorward via subtropical ocean–atmosphere coupling to trigger ENSO events (Vimont et al., 2003). Recent studies suggest that these two mechanisms can trigger events at different locations to produce the Eastern Pacific and Central Pacific types (Kao & Yu, 2009; Yu & Kao, 2007) of ENSO (Yu et al., 2010, 2012, 2017). However, it is not yet fully understood whether or not these two mechanisms impose any particular constraints on the event-to-event transitions and how they contribute to ENSO complexity.

In this study, we first show that the strengths of these two onset mechanisms can be determined from observations by applying a Multi-variate Empirical Orthogonal Function (MEOF) analysis to combined atmospheric and oceanic anomalies. The event-to-event transitions are then separately composited and analyzed for the two onset mechanisms using reanalysis products during the period 1958–2014. The same analyses are also performed with the preindustrial simulations produced by Climate Model Intercomparison Project version 5 (CMIP5) models (Taylor et al., 2012) to understand how simulations of these two onset mechanisms affect the properties of the model ENSOs.

## 2. Data Sets and Methods

Monthly mean values of SST, surface wind, and sea surface height (SSH) were used and regridded to a common  $1.5^\circ \times 1^\circ$  longitude-latitude grid for analysis. The SST data are from Hadley Center Sea Ice and Sea Surface Temperature data set (Rayner et al., 2003), the surface wind data are from the National Centers for Environmental Prediction-National Center for Atmospheric Research reanalysis (Kalnay et al., 1996), and the SSH data are from the German contribution of the Estimating the Circulation and Climate of the Ocean project (Köhl, 2015). Anomalies in this study are defined as the deviations from the seasonal cycle averaged over the analysis period after removing the linear trend. The same procedures were applied to the last 100 years of the preindustrial simulations produced by 34 CMIP5 models (see Table S1 in the supporting information for details).

To identify the dominant ocean-atmosphere coupling processes associated with ENSO, we applied an MEOF analysis to the combined anomalies of SST, surface wind, and SSH within the tropical Pacific ( $20^\circ\text{S}$ – $20^\circ\text{N}$ ,  $122^\circ\text{E}$ – $70^\circ\text{W}$ ) during the period 1958–2014. Following Xue et al. (2000), a two-step procedure was used to perform the MEOF analysis. The first step is to apply a spatial EOF analysis separately to the SST, wind, and SSH anomalies to obtain their individual leading EOF modes. The second step is to apply a temporal EOF analysis to the combined principal components (PCs) of the leading spatial EOF modes of each variable to obtain the leading coupled modes among the variables. The leading modes obtained from the final step of the MEOF analysis are referred to as the leading MEOF modes. The same MEOF analysis was applied to CMIP5 model simulations.

## 3. Results

Figure 1 shows the structures of the first three leading MEOF modes, which are similar to the MEOF modes obtained by Xue et al. (2000). The first mode (MEOF1) explains a large percentage (32%) of the coupled variance among surface wind, SST, and SSH. This mode represents the Bjerknes (BJ) feedback process that is well known as a positive feedback mechanism that can cause ENSO to grow in intensity (Bjerknes, 1969). This mode is characterized by warm SST anomalies in tropical central-to-eastern Pacific (Figure 1a) that are coupled with westerly anomalies to the west (Figure 1b) and an east-west sloping of thermocline (represented by SSH) along the tropical Pacific (Figure 1c).

The second mode (MEOF2; explaining 7.3% of variance) represents the SF mechanism and is characterized by positive SST anomalies extending from the subtropical northeastern Pacific into the equatorial central Pacific (Figure 1d) that assumes a pattern similar to the Pacific meridional mode (Chiang & Vimont, 2004). This meridional structure of SST anomalies is overlaid by surface southwesterly anomalies (Figure 1e) that are opposite in direction from the climatological trade winds. These anomalies thus weaken surface winds, reduce surface evaporation, and help maintain the positive Pacific meridional mode anomalies through the wind-evaporation-SST feedback (Xie & Philander, 1994). Meanwhile, the wind anomalies can deepen the thermocline in the central Pacific (Figure 1f), triggering the onset of an El Niño (Anderson & Perez, 2015). Conversely, the negative phase of the SF mechanism can trigger the onset of La Niña events (Yu & Kim, 2011).

The third mode (MEOF3; explaining 5.3% of the variance) represents the CD mechanism that is characterized by an increase in SSH (i.e., ocean heat content) along the entire equatorial Pacific and a decrease in SSH along most of an off-equatorial Pacific belt at about  $10^\circ\text{N}$  (Figure 1i). The increase (decrease) of the equatorial SSH, which represents the charging (positive) or discharging (negative) of the ocean heat content, is driven by the ENSO-associated wind anomalies in the tropical Pacific. The charging of the ocean heat content deepens the thermocline to onset positive SST anomalies in the tropical eastern Pacific (Figure 1g). The MEOF analysis clearly identifies one development mechanism (i.e., the BJ mechanism) and two onset mechanisms (the SF

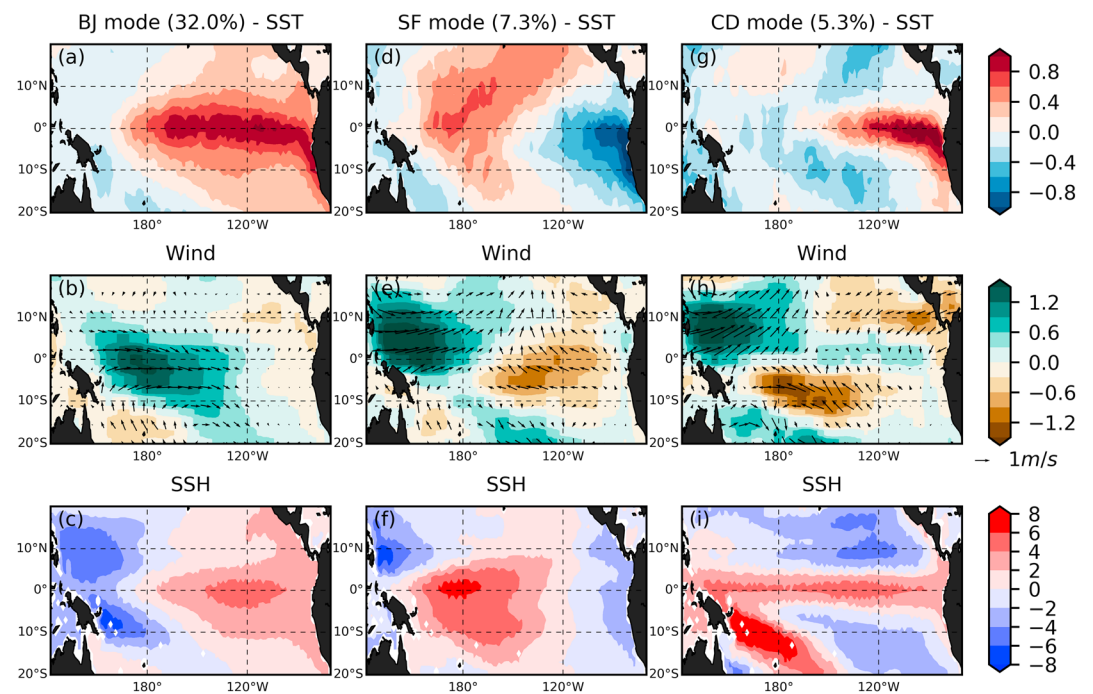


**Figure 1.** The anomaly patterns in (top row) sea surface temperatures, (middle row) surface winds, and (bottom row) sea surface heights associated with the Multi-variate Empirical Orthogonal Function (MEOF) modes for the (left column) Bjerknes mechanism (MEOF1), (middle column) seasonal footprinting mechanism (MEOF2), and (right column) charged-discharged mechanism (MEOF3).

and CD mechanisms) for ENSO. Although the second and third MEOF modes are not distinguishable from the higher modes based on the analysis of their eigenvalues (North, 1984), their robustness was examined by applying the same MEOF analyses separately to the first and second halves of the analysis period and using other sets of SST, SSH, and surface wind data (Balmaseda et al., 2013; Kobayashi et al., 2015; and Smith et al., 2008; see Text S1 in the supporting information). Similar first three MEOF modes were obtained in each of these additional analyses (Figures S4 and S3).

To confirm the relationships between the first three MEOF modes and ENSO, we performed a lead-lag correlation analysis between the PCs of the three modes and the Niño3.4 index (Figure S4). Being an ENSO development mechanism, the PC of the BJ mode (i.e., PC1) evolves together with the Niño3.4 with the largest correlation at lag 0. The PC of the SF mode (i.e., PC2) has its largest correlation with the Niño3.4 index when it leads Niño3.4 by about 9 months, indicating that the SF mode is an ENSO onset mechanism. The 9-month lead time is also consistent with the fact that the SF mechanism is usually at its strongest strength in boreal spring (Vimont et al., 2003), while ENSO typically peaks in boreal winter. The PC of the CD mode (i.e., PC3) has its largest positive correlation with Niño3.4 when it leads the index by 5–6 months and the largest negative correlation when it lags the index by 7–8 months. These two extreme values of correlation correspond to the charging (discharging) of ocean heat content before the El Niño (La Niña) onset and the discharging (charging) of the ocean heat content after the ENSO fully develops. A lead-lagged regression analysis of Pacific SST anomalies onto PC2 and PC3 also confirms that an ENSO event develops after the CD and SF modes peak (Figure S5).

To examine the degree of ENSO complexity produced by the CD and SF onset mechanisms, we performed a composite analysis that investigates the SST evolution associated with these two mechanisms. We first selected the months in which the PC2 (PC3) values are larger than one standard deviation for the composite of the positive SF (CD) mechanisms. Conversely, the months of negative SF (CD) mechanisms are chosen when the PC2 (PC3) values were smaller than  $-1$  standard deviation. Figures 2a–2d show the evolutions of the composited SST anomalies along the equatorial Pacific ( $5^{\circ}\text{S}$ – $5^{\circ}\text{N}$ ) during a period of 12 months before to 12 months after the peak of the two onset mechanisms.

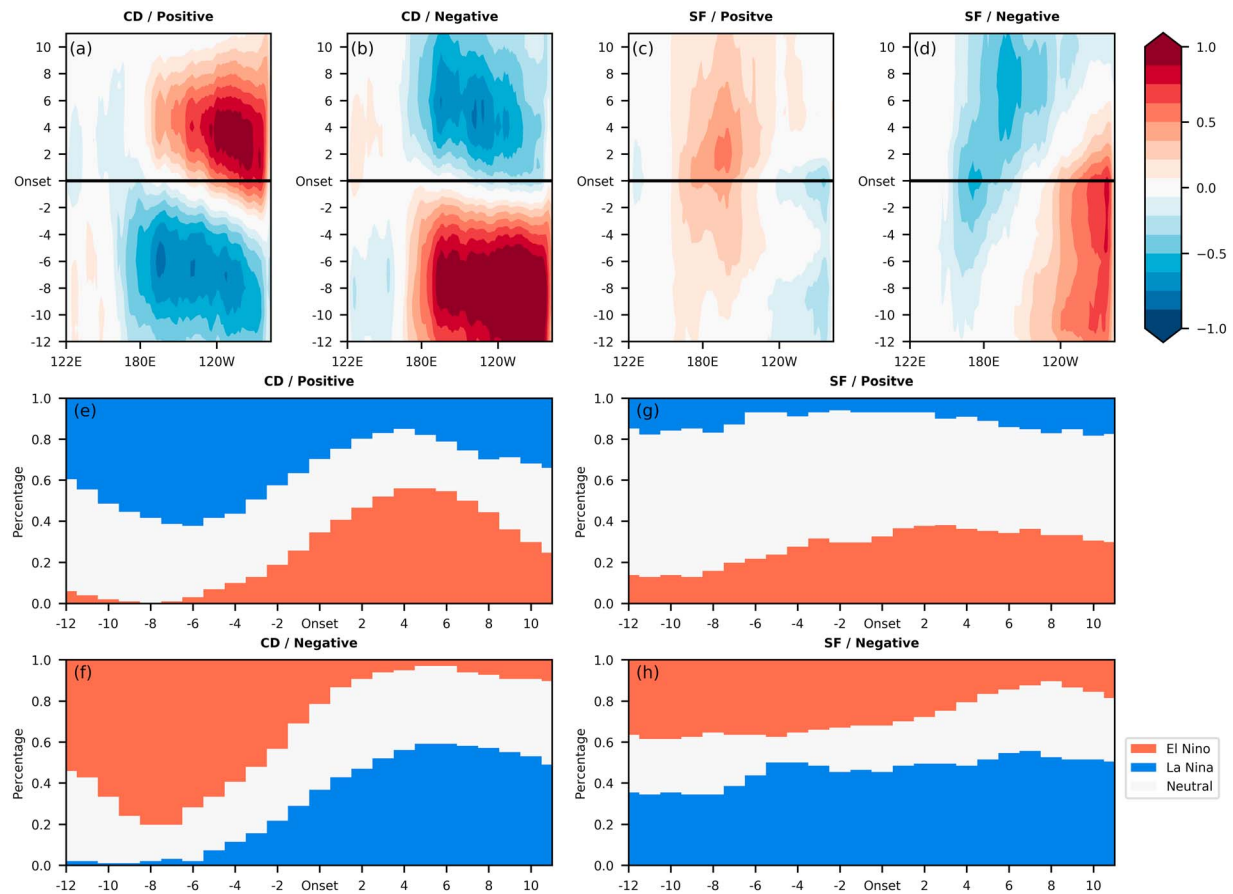


**Figure 2.** The evolution of equatorial Pacific (5°S–5°N) sea surface temperature anomalies composited for (a) the positive charged-discharged (CD) mechanism, (b) the negative CD mechanism, (c) the positive seasonal footprinting (SF) mechanism, and (d) the negative SF mechanism. (e–h) The percentages of the composited months that are in an El Niño (red), La Niña (blue), or neutral (white) state during the period 12 months before to 12 months after the positive and negative phases of the CD mode (e and f) and the SF mode (g and h) reach their peak (at lag 0). A composited month is determined to be in an El Niño (La Niña) state if the Niño3.4 index in that month is greater (smaller) than or equal to  $(-)$ 0.5°C. Otherwise, it is in a neutral state. The total number of months in each composite is shown above the upper-right corner of each panel.

The composite evolution for the CD mechanism (Figures 2a and 2b) is relatively simple and characterized by oscillatory transitions: A positive CD mode is preceded by a La Niña and followed by an El Niño event and vice versa for the negative CD mode. This is consistent with the existing view that a La Niña event produces a wind stress pattern that tends to charge the equatorial Pacific thermocline (i.e., a positive phase of the CD mechanism), which later onsets an El Niño event and vice versa for the negative CD mechanism. The evolution shows little asymmetry during ENSO transitions between positive and negative phases. It should be noted that previous studies have found that the charging associated with La Niña and the discharging associated with El Niño can be asymmetric in amplitude (Chen et al., 2015; Hu et al., 2017); however, this asymmetry differs from the transition asymmetry discussed here.

For the SF mechanism, the composite evolution is less oscillatory (Figures 2c and 2d). This is particularly clear for the positive SF mechanism, where the El Niño event it induces is not preceded by a La Niña. Also, the El Niño onset is in the tropical central Pacific rather than in the tropical eastern Pacific as is the case for the ENSO induced by the CD mechanism (cf. Figures 2a and 2b). As for the positive SF mechanism, the composite for the negative SF mechanism also shows that the La Niña develops in the tropical central Pacific with cold anomalies lingering in the region for many months before the onset. However, the evolution for the negative SF mechanism is not symmetric with respect to the positive SF mechanism. The negative SF composite is preceded by a strong El Niño, which has the magnitudes larger than the subsequent La Niña. We noticed that a number of the preceding months used in this composite are associated with the 1982–1983 and 1997–1998

El Niño events. Apparently, the ENSO evolution is very different between the positive and negative phases of the SF mechanism. The event-to-event evolution is more complex for the SF mechanism than for the CD mechanism and is also more asymmetric between the positive and negative phases of the SF mechanism.

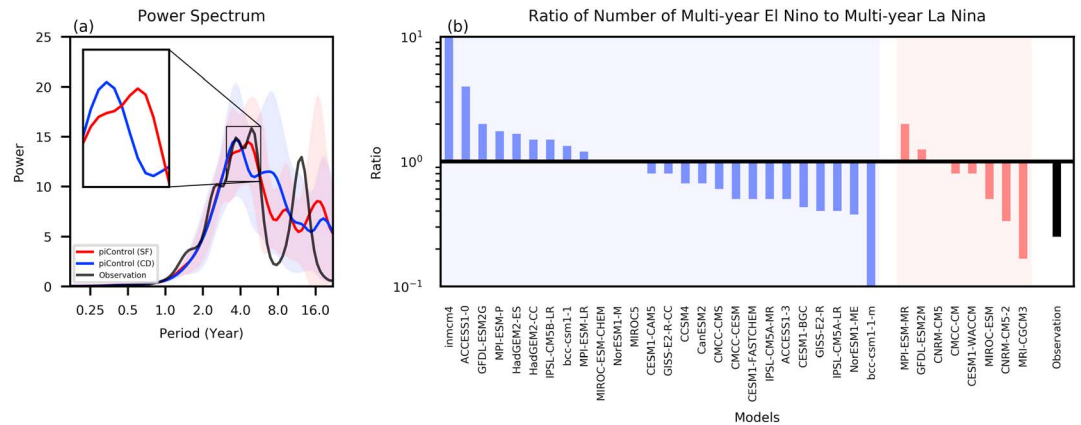
We performed another analysis with the same set of months selected for the composite SST analysis but focused on how the El Niño, La Niña, and neutral states evolve from one to another. A month is determined to be in an El Niño (La Niña) state if the Niño3.4 index in that month is greater (smaller) than or equal to  $(-)$ 0.5 °C. Otherwise, it is in a neutral state. We also used different thresholds (0.5, 0.8, and 1.0 standard deviation) to define strong onset mechanisms and found the composite results not sensitive to these thresholds (see Figure S6). Figure 2e shows the percentages of ENSO states before and after the positive CD mechanism peaks (i.e., at lag 0). The figure shows that, 5–6 months after the strong positive CD phase, close to 50% of the months are characterized by an El Niño state. The figure also indicates that the strong positive CD phase is preceded mostly ( $>60\%$ ) by a La Niña state. The composite for the strong negative CD phase (Figure 2f) shows a similar oscillatory evolution, except that the negative CD phase is preceded by an El Niño and followed by a La Niña. Figures 2e and 2f confirm that the CD onset mechanism strongly ( $>50\text{--}60\%$ ) regulates the transitions between El Niño and La Niña phases. Therefore, the CD onset mechanism acts to reduce ENSO complexity.

Figure 2g shows that a strong positive SF phase tends (about 40% of the time) to be followed by an El Niño state, as we expect from the SF mechanism (e.g., Chang et al., 2007; Yu et al., 2010). However, this SF phase is mostly ( $>80\%$ ) preceded by a neutral state. This is consistent with the understanding that the initial subtropical Pacific SST anomalies associated with the SF mechanism are often induced by subtropical or extratropical atmospheric disturbances, particularly the North Pacific Oscillation (NPO; Vimont et al., 2003; Yu & Kim, 2011). The NPO can be an internal mode of the atmosphere and is not necessarily forced by ENSO (Linkin & Nigam, 2008). Figure 2h shows that the negative SF phase tends (about 50%) to be followed by a La Niña state. Interestingly, the negative SF phase is mostly preceded by an El Niño (about 38%) or La Niña (51%) state but not the neutral state. The transition from a La Niña to another La Niña results in a multiyear La Niña event. That is, the negative phase of the SF mechanism is forced by ENSO, which is very different from the positive phase of the SF mechanism that is mostly not related to ENSO forcing.

The ENSO evolution revealed by Figures 2e–2h indicates that the CD onset mechanism tends to force ENSO to oscillate between the El Niño and La Niña phases, whereas no such a regulatory or oscillatory tendency exists for the SF onset mechanism. Therefore, the CD mechanism contributes to reduce the ENSO complexity, while the SF mechanism contributes to increase the ENSO complexity.

As noted in Figure 2h, the negative SF mechanism is often preceded by an El Niño or La Niña event. The preceding El Niño months are related to the extreme El Niño events, including the 1982–1983 and 1997–1998 El Niño events. Yu and Kim (2011) have shown that these extreme El Niño events can induce the positive phase of NPO via teleconnections to turn on the negative SF mechanism, which then onsets La Niña events in the tropical central Pacific. In fact, Figure 2h indicates that the negative SF onset mechanism is more often preceded by a La Niña event, resulting multiyear La Niña events. No such tendency for multiyear El Niño events can be found in the positive SF mechanism. All four multiyear La Niña events we identified (see Text S2 for a description of the methodology) in the analysis period maintained negative PC values of the SF mode throughout these events, but the PC values of the CD mode fluctuated from positive values in year 1 to negative values in year 2 (Figure S7). The asymmetry between the positive and negative phases of the SF mechanism is one possible reason why multiyear La Niña events occur more often than multiyear El Niño events (Hu et al., 2014; Ohba & Ueda, 2009; Okumura & Deser, 2010). The cause of this asymmetry associated with the positive and negative phases of the SF mechanism needs to be investigated but is beyond the scope of this study.

We next use the CMIP5 preindustrial simulations to examine two of our main findings so far: (1) That the SF mechanism increases ENSO complexity while the CD mechanism decreases complexity and (2) that the SF mechanism increases El Niño–La Niña asymmetries. Based on the eigenvalues of the CD and SF modes (Figure S8), we find that most (26 out of the 34) CMIP5 models are dominated by the CD onset mechanism. Only eight of the models are dominated by the SF onset mechanism. As the observation during the analysis period is dominated by the SF mechanism, this simple analysis indicates that contemporary climate models in general overestimate the strength of the CD onset mechanism but underestimate the strength of the SF



**Figure 3.** (a) Power spectrum of the normalized Niño3.4 index from observations (black), the multimodel mean of the seasonal footprinting (SF)-dominated (red), and the charged-discharged (CD)-dominated (blue) models from last hundred years of the preindustrial Climate Model Intercomparison Project version 5 simulations. The shading denotes one standard deviation of each spectrum. (b) The ratio of the number of multiyear El Niño events to the number of multiyear La Niña events. The y axis is in log<sub>10</sub> scale. The blue bars are used for the CD-dominated models, the red bars are used for the SF-dominated simulations, and the black bar is for the observations.

onset mechanism. Based on the observational composite analysis, we expect the models dominated by the CD onset mechanism to produce more regular and less complex ENSO evolutions compared to the models dominated by the SF mechanism. The power spectra of the Niño3.4 index produced by these two groups of models confirm this speculation. Figure 3 reveals that the mean spectrum averaged from all the CD-dominated models shows a sharp peak in power centered around 3–4 years indicating a very regular ENSO evolution, whereas the mean spectrum of the SF-dominated models shows large values of the power spread out over 2 to 6 years indicating a less-regular and more-complex evolution of their simulated ENSOs.

We also compared the El Niño-La Niña asymmetries between these two model groups by examining the ratio of the number of multiyear El Niño events to the number of multiyear La Niña events in the preindustrial simulations. Figure 3b shows that most (six out of eight) of the SF-dominated models show a ratio that

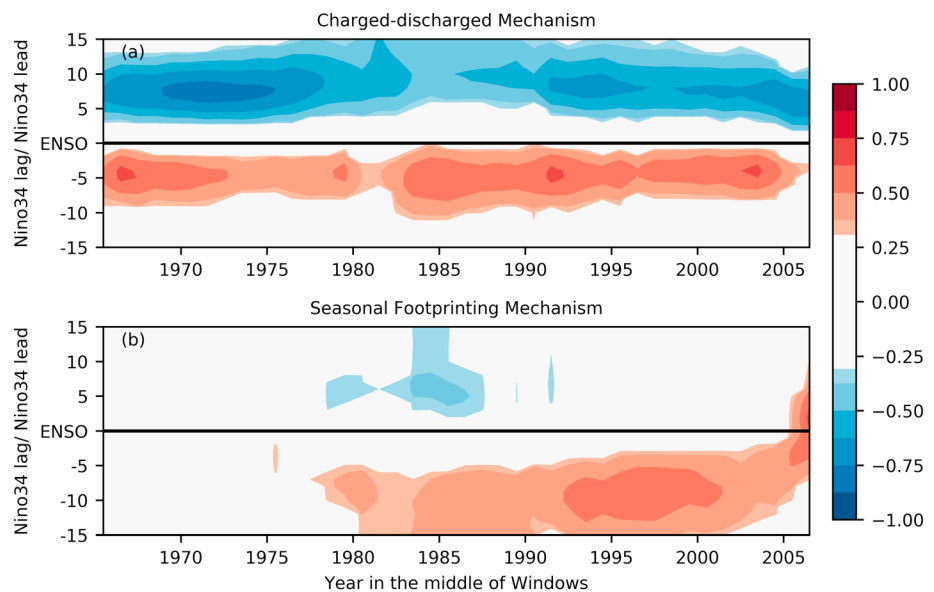


**Figure 4.** Fifteen-year sliding lead/lag correlation values between the Niño 3.4 index and (a) the principal components of the charged-discharged mode and (b) the seasonal footprinting mode. The color shaded areas are statistically significant at the 95% confidence level.

indicates a preference for more multiyear La niñas than El Niños. In contrast, the CD-dominated models do not show a preference of having more multiyear El Niño or La Niña events. This result adds some support to the notion that the SF mechanism can increase the El Niño-La Niña asymmetries.

We performed a 15-year sliding lead-lagged correlation between the PCs of the CD and SF modes constructed from the observations and the Niño3.4 index to examine the decadal variations of these two onset mechanisms. As shown in Figure 4, the CD mechanism has maintained a relatively stationary correlation with the Niño3.4 index throughout the past six decades, showing positive values when the CD mode leads the Niño3.4 index and negative values when the CD mode lags the Niño3.4. This result indicates that the strength or the contribution of the CD mechanism to ENSO does not exhibit any strong decadal variations during this period. In contrast, the correlation of the SF mechanism with the Niño3.4 index is weak before 1980, which means that the SF onset mechanism has become important only recently. The correlation intensified in particular after the early 1990s, which implies that ENSO complexity may have become more prominent during the last two decades. This is consistent with Yu et al. (2015), who reported that the SF mechanism intensified after the Atlantic Multidecadal Oscillation switched from a negative to a positive phase in the early 1990s. Lyu and Yu (2017) showed that a positive phase of the Atlantic Multidecadal Oscillation can intensify the eastern Pacific subtropical high enhancing the wind-evaporation-SST feedback strengthening the SF mechanism. Figure 4, in fact, also implies that the SF onset mechanism is more sensitive than the CD onset mechanism to changes in Pacific mean state. We note that the SF mechanism may have also changed after 2005, but since this change occurs toward the end of the period examined, more data are needed to confirm this change.

#### 4. Summary and Discussion

In this paper, we examined how the onset mechanisms can affect the ENSO complexity. We showed that the SF onset mechanism is a key source of ENSO complexity and is also capable of importing extratropical influences that can produce multiyear La Niña events as well as El Niño-La Niña asymmetries, a finding that has not previously been emphasized. Our results are consistent with the existing view that stochastic forcing from the extratropics can increase ENSO irregularity (e.g., Alexander et al., 2010; Chang et al., 1996) and diversity (e.g., Capotondi et al., 2015), but we are able to additionally and more specifically describe how the extratropical stochastic forcing works through the SF mechanism to increase ENSO complexity. The analyses of the two onset mechanisms shed light on the possible sources/causes of the ENSO complexity, which may enable us to better project future changes in ENSO. Our results also indicate that by examining the two ENSO onset mechanisms, we are able to explain the ENSO properties found in a large number of climate models in a novel way.

#### References

- Alexander, M. A., Vimont, D. J., Chang, P., & Scott, J. D. (2010). The impact of extratropical atmospheric variability on ENSO: Testing the seasonal footprinting mechanism using coupled model experiments. *Journal of Climate*, 23(11), 2885–2901. <https://doi.org/10.1175/2010JCLI3205.1>
- Anderson, B. T., & Perez, R. C. (2015). ENSO and non-ENSO induced charging and discharging of the equatorial Pacific. *Climate Dynamics*, 45(9–10), 2309–2327. <https://doi.org/10.1007/s00382-015-2472-x>
- Balmaseda, M. A., Mogensen, K., & Weaver, A. T. (2013). Evaluation of the ECMWF ocean reanalysis system ORAS4. *Quarterly Journal of the Royal Meteorological Society*, 139(674), 1132–1161. <https://doi.org/10.1002/qj.2063>
- Bjerknes, J. (1969). Atmospheric teleconnections from the equatorial Pacific 1. *Monthly Weather Review*, 97(3), 163–172. [https://doi.org/10.1175/1520-0493\(1969\)097<0163:ATFTEP>2.3.CO;2](https://doi.org/10.1175/1520-0493(1969)097<0163:ATFTEP>2.3.CO;2)
- Capotondi, A., Wittenberg, A. T., Newman, M., Di Lorenzo, E., Yu, J. Y., Braconnot, P., et al. (2015). Understanding ENSO diversity. *Bulletin of the American Meteorological Society*, 96(6), 921–938. <https://doi.org/10.1175/BAMS-D-13-00117.1>
- Chang, P., Ji, L., Li, H., & Flugel, M. (1996). Chaotic dynamics versus stochastic processes in El Niño–Southern Oscillation in coupled ocean-atmosphere models. *Physica D*, 98(2–4), 301–320. [https://doi.org/10.1016/0167-2789\(96\)00116-9](https://doi.org/10.1016/0167-2789(96)00116-9)
- Chang, P., Zhang, L., Saravanan, R., Vimont, D. J., Chiang, J. C. H., Ji, L., et al. (2007). Pacific meridional mode and El Niño–Southern Oscillation. *Geophysical Research Letters*, 34, L16608. <https://doi.org/10.1029/2007GL030302>
- Chen, H. C., Sui, C. H., Tseng, Y. H., & Huang, B. (2015). An analysis of the linkage of Pacific subtropical cells with the recharge-discharge processes in ENSO evolution. *Journal of Climate*, 28(9), 3786–3805. <https://doi.org/10.1175/JCLI-D-14-00134.1>
- Chiang, J. C., & Vimont, D. J. (2004). Analogous Pacific and Atlantic meridional modes of tropical atmosphere-ocean variability. *Journal of Climate*, 17(21), 4143–4158. <https://doi.org/10.1175/JCLI4953.1>
- Hu, Z. Z., Kumar, A., Huang, B., Zhu, J., Zhang, R. H., & Jin, F. F. (2017). Asymmetric evolution of El Niño and La Niña: The recharge/discharge processes and role of the off-equatorial sea surface height anomaly. *Climate Dynamics*, 49(7–8), 2737–2748. <https://doi.org/10.1007/s00382-016-3498-4>

#### Acknowledgments

We thank two anonymous reviewers and Editor Meghan Cronin for their valuable comments. This research is supported by NSF Climate & Large-scale Dynamics Program under grant AGS-1505145. The SST data of Hadley Center Sea Ice and Sea Surface Temperature data set were downloaded from their site (<http://www.metoffice.gov.uk/hadobs/hadisst/data/download.html>), and the NOAA Extended Reconstructed SST V3 and the wind field of National Centers for Environmental Prediction/National Center for Atmospheric Research were from NOAA (<https://www.esrl.noaa.gov/psd/>). The wind of Japanese 55-year Reanalysis project is carried out by the Japan Meteorological Agency. Both SSH data sets of German contribution of the Estimating the Circulation and Climate of the Ocean project and Ocean Reanalysis System 4 were downloaded from the Integrated Climate Data Center (<http://icdc.cen.uni-hamburg.de/projekte/easy-init/easy-init-ocean.html>). We acknowledge the World Climate Research Programme's Working Group on Coupled Modeling, which is responsible for CMIP, and we thank the climate modeling groups (listed in Table S1 of this paper) for producing and making available their model output. For CMIP the U.S. Department of Energy's Program for Climate Model Diagnosis and Intercomparison provides coordinating support and led development of software infrastructure in partnership with the Global Organization for Earth System Science Portals.

- Hu, Z. Z., Kumar, A., Xue, Y., & Jha, B. (2014). Why were some La Niñas followed by another La Niña? *Climate Dynamics*, 42(3–4), 1029–1042. <https://doi.org/10.1007/s00382-013-1917-3>
- Jin, F. F. (1997a). An equatorial ocean recharge paradigm for ENSO. Part I: Conceptual model. *Journal of the Atmospheric Sciences*, 54(7), 811–829. [https://doi.org/10.1175/1520-0469\(1997\)054<0811:AEORPF>2.0.CO;2](https://doi.org/10.1175/1520-0469(1997)054<0811:AEORPF>2.0.CO;2)
- Jin, F. F. (1997b). An equatorial ocean recharge paradigm for ENSO. Part II: A stripped-down coupled model. *Journal of the Atmospheric Sciences*, 54(7), 830–847. [https://doi.org/10.1175/1520-0469\(1997\)054<0830:AEORPF>2.0.CO;2](https://doi.org/10.1175/1520-0469(1997)054<0830:AEORPF>2.0.CO;2)
- Kalnay, E., Kanamitsu, M., Kistler, R., Collins, W., Deaven, D., Gandin, L., et al. (1996). The NCEP/NCAR 40-year reanalysis project. *Bulletin of the American Meteorological Society*, 77(3), 437–471. [https://doi.org/10.1175/1520-0477\(1996\)077<0437:TNYRP>2.0.CO;2](https://doi.org/10.1175/1520-0477(1996)077<0437:TNYRP>2.0.CO;2)
- Kao, H. Y., & Yu, J. Y. (2009). Contrasting eastern-Pacific and central-Pacific types of ENSO. *Journal of Climate*, 22(3), 615–632. <https://doi.org/10.1175/2008JCLI2309.1>
- Kobayashi, S., Ota, Y., Harada, Y., Ebata, A., Moriya, M., Onoda, H., et al. (2015). The JRA-55 reanalysis: General specifications and basic characteristics. *Journal of the Meteorological Society of Japan. Ser. II*, 93(1), 5–48.
- Köhl, A. (2015). Evaluation of the GECCO2 ocean synthesis: Transports of volume, heat and freshwater in the Atlantic. *Quarterly Journal of the Royal Meteorological Society*, 141(686), 166–181. <https://doi.org/10.1002/qj.2347>
- Linkin, M. E., & Nigam, S. (2008). The North Pacific Oscillation-west Pacific teleconnection pattern: Mature-phase structure and winter impacts. *Journal of Climate*, 21(9), 1979–1997. <https://doi.org/10.1175/2007JCLI2048.1>
- Lyu, K., & Yu, J.-Y. (2017). Climate impacts of the Atlantic Multidecadal Oscillation simulated in the CMIP5 models: A re-evaluation based on a revised index. *Geophysical Research Letters*, 44(8), 3867–3876. <https://doi.org/10.1002/2017GL072681>
- North, G. R. (1984). Empirical orthogonal functions and normal modes. *Journal of the Atmospheric Sciences*, 41(5), 879–887. [https://doi.org/10.1175/1520-0469\(1984\)041<0879:EOFANM>2.0.CO;2](https://doi.org/10.1175/1520-0469(1984)041<0879:EOFANM>2.0.CO;2)
- Ohba, M., & Ueda, H. (2009). Role of nonlinear atmospheric response to SST on the asymmetric transition process of ENSO. *Journal of Climate*, 22(1), 177–192. <https://doi.org/10.1175/2008JCLI2334.1>
- Okumura, Y. M., & Deser, C. (2010). Asymmetry in the duration of El Niño and La Niña. *Journal of Climate*, 23(21), 5826–5843. <https://doi.org/10.1175/2010JCLI3592.1>
- Rayner, N. A., Parker, D. E., Horton, E. B., Folland, C. K., Alexander, L. V., Rowell, D. P., et al. (2003). Global analyses of sea surface temperature, sea ice, and night marine air temperature since the late nineteenth century. *Journal of Geophysical Research*, 108(D14), 4407. <https://doi.org/10.1029/2002JD002670>
- Smith, T. M., Reynolds, R. W., Peterson, T. C., & Lawrimore, J. (2008). Improvements to NOAA's historical merged land-ocean surface temperature analysis (1880–2006). *Journal of Climate*, 21(10), 2283–2296. <https://doi.org/10.1175/2007JCLI2100.1>
- Taylor, K. E., Stouffer, R. J., & Meehl, G. A. (2012). An overview of CMIP5 and the experiment design. *Bulletin of the American Meteorological Society*, 93(4), 485–498. <https://doi.org/10.1175/BAMS-D-11-00094.1>
- Vimont, D. J., Wallace, J. M., & Battisti, D. S. (2003). The seasonal footprinting mechanism in the Pacific: Implications for ENSO. *Journal of Climate*, 16(16), 2668–2675. [https://doi.org/10.1175/1520-0442\(2003\)016<2668:TSFMIT>2.0.CO;2](https://doi.org/10.1175/1520-0442(2003)016<2668:TSFMIT>2.0.CO;2)
- Wang, C., Deser, C., Yu, J. Y., DiNezio, P., & Clement, A. (2017). El Niño and Southern Oscillation (ENSO): A review. In *Coral reefs of the eastern tropical Pacific* (pp. 85–106). Netherlands: Springer. [https://doi.org/10.1007/978-94-017-7499-4\\_4](https://doi.org/10.1007/978-94-017-7499-4_4)
- Wyrtki, K. (1975). El Niño—The dynamic response of the equatorial Pacific Ocean to atmospheric forcing. *Journal of Physical Oceanography*, 5(4), 572–584. [https://doi.org/10.1175/1520-0485\(1975\)005<0572:ENTDRO>2.0.CO;2](https://doi.org/10.1175/1520-0485(1975)005<0572:ENTDRO>2.0.CO;2)
- Xie, S. P., & Philander, S. G. H. (1994). A coupled ocean-atmosphere model of relevance to the ITCZ in the eastern Pacific. *Tellus A*, 46(4), 340–350. <https://doi.org/10.3402/tellusa.v46i4.15484>
- Xue, Y., Leetmaa, A., & Ji, M. (2000). ENSO prediction with Markov models: The impact of sea level. *Journal of Climate*, 13(4), 849–871. [https://doi.org/10.1175/1520-0442\(2000\)013<0849:EPWMMT>2.0.CO;2](https://doi.org/10.1175/1520-0442(2000)013<0849:EPWMMT>2.0.CO;2)
- Yu, J. Y., & Kao, H. Y. (2007). Decadal changes of ENSO persistence barrier in SST and ocean heat content indices: 1958–2001. *Journal of Geophysical Research*, 112, D13106. <https://doi.org/10.1029/2006JD007654>
- Yu, J. Y., Kao, P. K., Paek, H., Hsu, H. H., Hung, C. W., Lu, M. M., & An, S. I. (2015). Linking emergence of the central Pacific El Niño to the Atlantic Multidecadal Oscillation. *Journal of Climate*, 28(2), 651–662. <https://doi.org/10.1175/JCLI-D-14-00347.1>
- Yu, J. Y., & Kim, S. T. (2011). Relationships between extratropical sea level pressure variations and the central Pacific and eastern Pacific types of ENSO. *Journal of Climate*, 24(3), 708–720. <https://doi.org/10.1175/2010JCLI3688.1>
- Yu, J.-Y., Wang, X., Yang, S., Paek, H., & Chen, M. (2017). In S.-Y. Wang, J.-H. Yoon, C. Funk, & R. R. Gillies (Eds.), *Changing El Niño—Southern Oscillation and associated climate extremes, book chapter in climate extremes: Patterns and mechanisms, Geophysical Monograph Series* (Vol. 226, pp. 3–38). Washington, DC: American Geophysical Union.
- Yu, J.-Y., Kao, H.-Y., & Lee, T. (2010). Subtropics-related interannual sea surface temperature variability in the equatorial central Pacific. *Journal of Climate*, 23(11), 2869–2884. <https://doi.org/10.1175/2010JCLI3171.1>
- Yu, J.-Y., Lu, M.-M., & Kim, S. T. (2012). A change in the relationship between tropical central Pacific SST variability and the extratropical atmosphere around 1990. *Environmental Research Letters*, 7(3), 034025. <https://doi.org/10.1088/1748-9326/7/3/034025>